Analysis of Non-Minimum Phase Behavior of PEM Fuel Cell Membrane Humidification Systems

Dongmei Chen Huei Peng[1]
Department of Mechanical Engineering
University of Michigan, Ann Arbor, MI 48109-2125

***Abstract*—A model for the transient behavior of a membrane humidifier for PEM fuel cells is developed. This humidifier uses the exhaust fuel cell cooling water to humidify the dry inlet air. This model is based on thermodynamic principles and captures temperature, relative humidity and flow variables of the humidifier. Dynamic simulations show that the humidification system exhibits a non-minimum phase behavior with one zero located in the right half plane. The physical reason why such a non-minimum phase zero exists is explained. The effects of the humidifier design parameters on the non-minimum phase zero location are studied and discussed.**

I. Introduction

The current generation of low-temperature Proton Exchange Membrane Fuel Cells (PEMFCs) work well only when the membrane humidity is properly controlled. The PEMFC membrane humidity is affected by the membrane properties, water generated during the fuel cell operation, the stack temperature, and the inlet reactants' humidity condition. The membrane properties are fixed once the fuel cell is designed and thus is not manipulatable in real-time. The water generated during the operation is a function of the stack current and cannot be changed freely. Finally, the fuel cell temperature is usually kept around 80-90°C. Therefore, only the inlet reactants humidity conditions can be changed freely to influence the membrane humidity. In order to achieve optimum performance during transients, a properly controlled humidifier at the PEMFC inlet is required. A humidifier can be installed upstream of the fuel cell stack to change the reactants humidity. To design the humidifier control algorithm properly, we first need to develop a dynamic humidifier model.

Fuel cell water management was actively investigated in the literature. A number of experimental studies were conducted to understand the water transport phenomena and to characterize the factors that affect the membrane water content [1-4]. Innovative channel designs have been proposed to better maintain the humidity [5, 6]. A number of mathematic models have been developed to optimize the fuel cell design to maintain high humidity [7-14]. In addition, several types of humidifiers have been designed and analyzed to enhance the stack humidity [15-18]. The main purpose of these works is either to understand the system or to size the components. Few dynamic models suitable for control design purposes exist.

A four-state thermodynamic model of a membrane humidifier is developed in [19]. This model captures the dynamics of flow rate, temperature, pressure and relative humidity. This paper is a continuation of [19] and is focused on the analysis of the humidifier dynamic response, with the emphasis on its non-minimum phase characteristics. The impact of the humidifier design parameters on the non-minimum phase zero location is subsequently studied which may be instrumental in the design of future PEMFC humidifier systems.

II. Humidification System Modeling

A dynamic model for a membrane-based humidifier system was developed by the authors in an earlier paper [19]. This humidifier system uses the exhaust cooling water from the PEMFC stack to humidify the dry inlet air. The water and the dry air flow in two sides of a Nafion® membrane, which allows water vapor transfer from the water side to the gas side. The vapor transfer rate is determined by the water and gases flow rates (convective driving force), membrane pressure differential (diffusive driving force), membrane thickness, and fluid temperatures. The schematic diagram of a humidifier unit is shown in Fig. 1. There are three channels in each humidifier unit: the humidification channel marked with 'A', a heat transfer channel marked with 'B', and the water channel marked with 'C'. The dry inlet air can be directed to go through either channel 'A' or channel 'B'. When the inlet air passes through channel 'A', both heat and water vapor exchanges with channel 'C' will occur. On the contrary, when the air passes through channel 'B', only heat exchange will happen. Depending on the position of the sliding plate, the air will be directed to go through either channel 'A' to be humidified, or channel 'B' to be heated only.

Based on the size and load of the fuel cell stack, the size and number of humidifier units can be calculated. Assuming there are *N* humidifier units, the number of units designated as type 'A' is denoted as *'n'*, which can be any

[1]Corresponding author, Associate Professor, Department of Mechanical Engineering, University of Michigan, Ann Arbor, MI 48109-2133, 734-936-0352, hpeng@umich.edu

® Nafion is a trademark of DuPont Company

number between 0 and N, depending on the desired relative humidity of the exiting air. It should be noted that the authority of the humidifier in reducing humidity is limited (or non-existent, if heat exchange effect is ignores). For example, when the inlet air has a non-zero relative humidity, we will not be able to get 0% relative humidity at the outlet even through no channel 'A' is used.

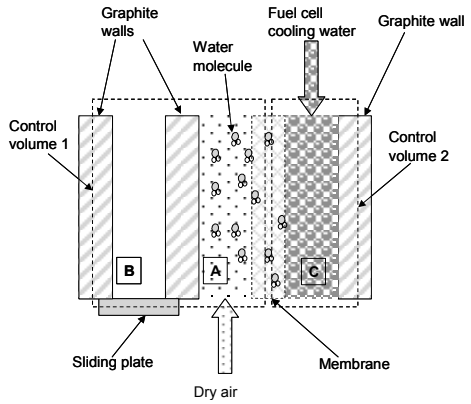

Fig. 1: Structure of one humidifier unit

In order to derive the modeling equations, two control volumes are defined as shown in Fig. 2. The air inlet mass flow rate, pressure, temperature, and relative humidity (RH) are denoted as $M_{1,in}$, $P_{1,in}$, $T_{1,in}$, and $\Phi_{1,in}$, and those for the outlet flow are $M_{1,out}$, $P_{1,out}$, $T_{1,out}$, and $\Phi_{1,out}$. Denote the water inlet mass rate, pressure, and temperature as $M_{2,in}$, $P_{2,in}$, and $T_{2,in}$, and those for the outlet as $M_{2,out}$, $P_{2,out}$, and $T_{2,out}$. Finally, the membrane vapor transfer rate is $\dot{m}_{v,tr}$.

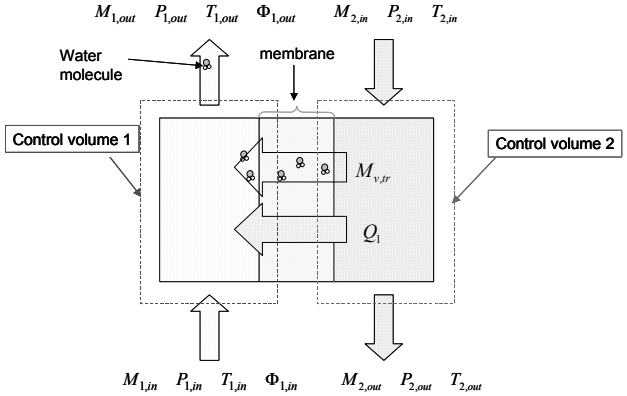

Fig. 2: Control volumes of one humidifier unit

The main equations used in [19] are summarized below. Apply the 1st law of thermodynamics to Control Volume 1, the energy equation is

$$\dot{m}_{a,1}u_{a,1}+\dot{m}_{v,1}u_{v,1}+m_{a,1}\dot{u}_{a,1}+m_{v,1}\dot{u}_{v,1}=\dot{Q}_1+\dot{m}_{a,in}h_{a,in}+\dot{m}_{v,in}h_{v,in}+\dot{m}_{v,tr}h_{mem}-\dot{m}_{a,out}h_{a,out}-\dot{m}_{v,out}h_{v,out} \quad (1)$$

$$u_{k1,1}=\int Cv_{k1}\dot{T}_{1,out} \qquad h_{k1,k2}=\int Cp_{k1}\dot{T}_{1,k2} \qquad h_{v,tr}=\int Cp_v\dot{T}_{mem}$$

where Cv_a, Cv_v, Cp_a, Cp_v are the specific heats of the air and vapor, subscript *k1* is *a* or *v*, for air or vapor, *k2=in* or *out,* representing inlet and outlet, subscript *1* represents Control Volume 1, *tr* represents membrane transfer. It is also assumed that T_{mem} equals $T_{2,in}$.

Apply the 1st law of thermodynamics to Control Volume 2, the energy equation is

$$m_{w,2}Cp_w\dot{T}_{2,out}=-\dot{Q}_1+\dot{m}_{2,in}h_{w,in}-\dot{m}_{2,out}h_{w,out}-\dot{m}_{v,tr}h_{mem}$$
$$h_{w,k2}=\int Cp_w\dot{T}_{2,k2} \quad (2)$$

where Cp_w is the specific heat of water. Subscript *w* represents water, and *2* represents Control Volume 2. $\dot{m}_{a,1}$ and $\dot{m}_{v,1}$ are calculated from

$$\dot{m}_{a,1}=\dot{m}_{a,in}-\dot{m}_{a,out} \quad (3)$$

$$\dot{m}_{v,1}=\dot{m}_{v,in}+\dot{m}_{v,tr}-\dot{m}_{v,out} \quad (4)$$

$$\dot{m}_{1,k2}=\dot{m}_{a,k2}+\dot{m}_{v,k2} \quad (5)$$

$$\omega_{1,k2}=\frac{M_v}{M_{air}}\frac{P_{v,k2}}{P_{a,k2}} \quad (6)$$

$$\dot{m}_{a,k2}=\frac{1}{1+\omega_{1,k2}}\dot{m}_{k2,1} \quad (7)$$

$\dot{m}_{1,out}$ can be calculated from

$$\dot{m}_{1,out}=Cr_1\sqrt{P_{1,out}-P_{fc,in}} \quad (8)$$

where $P_{fc,in}$ is the fuel cell inlet pressure, and Cr_1 is the nozzle constant which changes with orifice size and the gas density and can be obtained through experiments. $\dot{m}_{w,2}$ can be calculated as

$$\dot{m}_{w,2}=\dot{m}_{2,in}-\dot{m}_{v,tr}-\dot{m}_{2,out} \quad (9)$$

The total vapor transfer through the membrane $\dot{m}_{v,tr}$ is obtained from

$$\dot{m}_{v,tr}=D_w\frac{C_2-C_1}{t_m}M_vA \qquad D_w=D_\lambda e^{(2416(\frac{1}{303}-\frac{1}{Tw}))} \quad (10)$$

where D_W is the membrane coefficient of diffusion. C_2 and C_1 are water concentrations of the membrane on the air side and the water side, and are defined in Eq. (12). t_m is the membrane thickness. T_w is the membrane temperature. M_v is the vapor molar mass. A is the mass transfer area. The coefficient D_λ is determined empirically and has a piecewise-linear form [7]

$$D_\lambda = \begin{cases} 10^{-6} & \lambda < 2 \\ 10^{-6}(1+2(\lambda-2)) & 2 \le \lambda \le 3 \\ 10^{-6}(3-1.67(\lambda-3)) & 3 < \lambda < 4.5 \\ 1.25*10^{-6} & \lambda \ge 4.5 \end{cases} \quad (11)$$

The water concentrations are

$$C_1 = \frac{\rho_{m,dry}}{M_{m,dry}}\lambda_1 \qquad C_2 = \frac{\rho_{m,dry}}{M_{m,dry}}\lambda_2 \quad (12)$$

where $\rho_{m,dry}$ is the membrane dry density and $M_{m,dry}$ is the membrane dry equivalent weight. Water content λ_1 and λ_2 are calculated from

$$\lambda_1 = (0.043 + 17.81a_1 - 39.85a_1^2 + 36.0a_1^3) \quad a_1 = \frac{P_{v,1}}{P_{sat,1}} \quad (13)$$

$$\lambda_2 = 14$$

where $P_{v,1}$ is the vapor partial pressure of Control Volume 1. $P_{sat,1}$ is the saturation pressure of Control Volume 1, and is determined by

$$\log_{10}(P_{sat,1}) = 2.95 \cdot 10^{-2} T_{a,out} - 9.18 \cdot 10^{-5} T_{a,out}^2 + 1.44 \cdot 10^{-7} T_{a,out}^2 - 2.18 \quad (14)$$

The vapor partial pressure of Control Volume 1 is obtained from the ideal gas law.

$$P_{v,1}V_{c1} = R_v T_1 m_{v,1} \quad (15)$$

$$P_{a,1}V_{c1} = R_a T_1 m_{a,1} \quad (16)$$

$$P_{1,k2} = P_{v,k2} + P_{a,k2} \quad (17)$$

where R_a and R_v are the air and vapor gas constant, V_{c1} is the volume of Control Volume 1, $P_{a,1} = P_{a,out}$, $P_{v,1} = P_{v,out}$.

The heat transfer rate can be calculated from

$$\dot{Q}_1 = UA\Delta T_{2/1} \quad (18)$$

where A is the heat transfer area, U is the heat transfer coefficient defined as

$$U = \frac{1}{(1/h_1 + 1/h_2)} \quad h_1 = Nu_D \frac{k_a}{D_h} \quad h_2 = Nu_D \frac{k_w}{D_h} \quad (19)$$

where k_a and k_w are the air and water thermal conductivities, Nu_D is Nusselt number and D_h is the channel hydraulic diameter. $\Delta T_{2/1}$ is the temperature difference between the water and the gas. For counter flow,

$$\Delta T_{2/1} = \frac{(T_{2,in} - T_{1,out}) - (T_{2,out} - T_{1,in})}{\ln((T_{2,in} - T_{1,out})/(T_{2,out} - T_{1,in}))} \quad (20)$$

The model is summarized as follows. The states are: $x = \begin{bmatrix} m_{a,1} & m_{v,1} & T_{1,out} & T_{2,out} \end{bmatrix}^T$. Possible measurements include: $y = \begin{bmatrix} \dot{Q}_1 & \dot{m}_{v,tr} & \dot{m}_{1,out} & P_{1,out} & \Phi_{1,out} & \dot{m}_{2,out} \end{bmatrix}^T$. The control input is: $u = \frac{1}{N}[n]$. The performance variable is: $z = \begin{bmatrix} \dot{m}_{v,tr} \end{bmatrix}$, and the external disturbances include: $w = \begin{bmatrix} \dot{m}_{1,in} & T_{1,in} & P_{1,in} & \Phi_{1,in} & P_{2,in} & P_{2,out} & T_{2,in} \end{bmatrix}^T$

II. Dynamic Simulation Results

The model presented in the previous section is implemented in the Matlab/Simulink environment. Among the external disturbances of the humidifier system, the most important ones are inlet air flow rate, temperature and RH. The open-loop behaviors of the humidifier under the three disturbances are presented below. Fig. 3 shows that when there is a step increase in the inlet air flow rate, the membrane vapor transfer rate increases, while outlet RH decreases at steady-state. The total vapor rate is the sum of the membrane vapor transfer rate and the inlet vapor rate, which represents the amount of water content going into the fuel cell cathode. Interestingly, all the three response signals exhibit a non-minimum-phase behavior, which has important implications on the overall control system design—we will come back to this important phenomenon later.

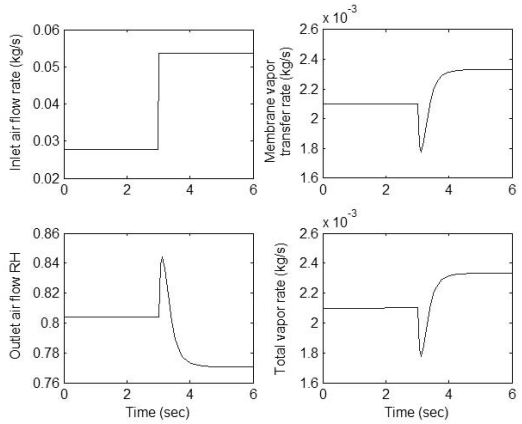

Fig. 3: System responses under a step increase of the inlet airflow rate

Fig. 4 shows that when there is a step decrease in the inlet air temperature, the membrane vapor transfer rate decreases and the outlet RH increases slightly at steady state. More importantly, all the three response signals exhibit an overshoot behavior that is quite unusual in thermodynamic systems.

Fig. 5 shows that when there is a step increase in the inlet air RH, the membrane vapor transfer rate decreases. This is due to the fact that the membrane vapor transfer rate, as described in Eq.(10), is a function of the RH difference across the membrane. When the inlet air RH

increases, the RH gradient across the membrane decreases, therefore, the membrane vapor transfer rate reduces. However, there is little change of the total vapor rate because the membrane vapor transfer rate decrease is compensated by the inlet air RH increase. For the same reason, there is little change of the outlet RH before and after the step disturbance.

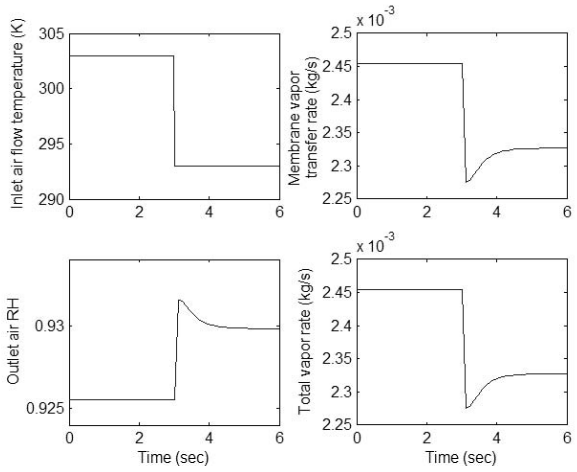

Fig. 4: System responses under a step decrease of the inlet air temperature

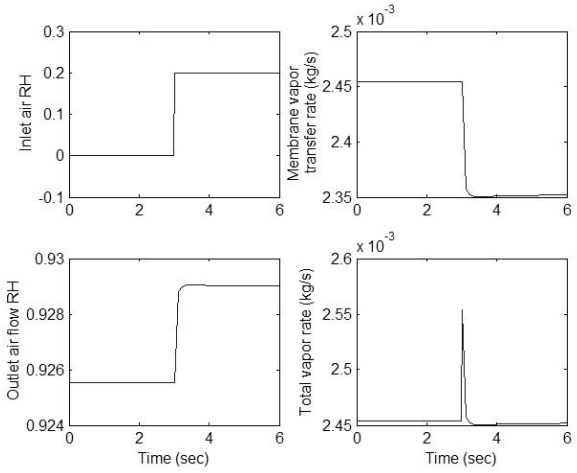

Fig. 5: System responses under a step increase of the inlet air RH

In Fig. 3 and Fig. 4, there are no other sources of vapor going into the system; the change in total vapor rate is completely due to the change in membrane vapor transfer rate. However, in Fig. 5, due to the inlet RH increases, the inlet vapor rate increases. The total vapor rate goes into the system equals the membrane vapor transfer rate plus the inlet vapor rate.

III. Non-Minimum-Phase Zero Analysis

Fig. 3 shows that the membrane vapor transfer rate exhibits a non-minimum-phase (NMP) behavior when the inlet air mass flow rate changes. NMP is an interesting and important phenomenon because of the implied closed-loop performance limit. This NMP zero is caused by the lag in vapor mass rate response, $\dot{m}_{v,1}$, which is explained below. The membrane vapor transfer rate is a function of air outlet RH Φ, which is defined as

$$\Phi = \frac{P_{v,out}}{P_{sat}} \tag{21}$$

Substitute $P_{sat} = f(T_{1,out})$ and $P_{v,out} = \frac{m_{v,1} R_{vapor} T_{1,out}}{V_{volume}}$, Eqn. (21) becomes

$$\Phi = \frac{m_{v,1} R_{vapor} T_{1,out}}{f(T_{1,out}) V_{volume}} \tag{22}$$

Define $C_\Phi = \frac{R_{vapor}}{V_{volume}}$ and $gT = \frac{T_{1,out}}{f(T_{1,out})}$, Eq. (22) becomes

$$\Phi = C_\Phi m_{v,1} gT \tag{23}$$

The changing rate of the relative humidity is then

$$\dot{\Phi} = C_\Phi \left[\dot{m}_{v,1}\, gT + m_{v,1}\, \dot{gT} \right] \tag{24}$$

Eqn. (24) shows that $\dot{\Phi}$ is a function of $\dot{m}_{v,1}$, gT, $m_{v,1}$ and $\dot{gT}$. These four variables' responses under inlet air flow rate step increase are plotted in Fig. 6, where $\dot{m}_{v,1}\, gT$ is noted as "Element 1" and $m_{v,1}\, \dot{gT}$ is noted as "Element 2". Fig. 6 shows that Element 1 reaches its peak later than Element 2 does.

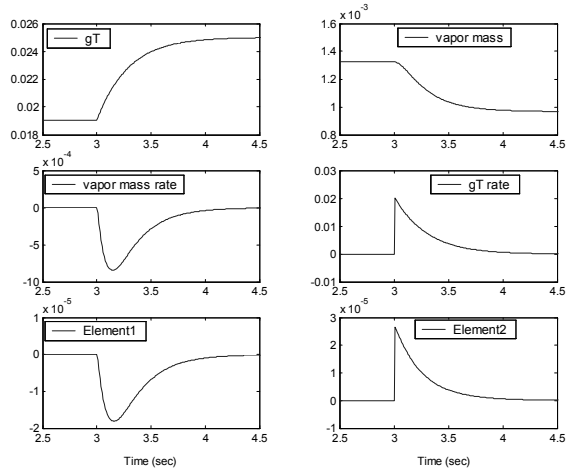

Fig. 6: System responses under an inlet air flow rate step increase

The responses of RH and RH rate under a step increase in the inlet air flow are shown in Fig. 7. It can be seen that $\dot{\Phi}$ is positive before t=3.1sec and negative afterwards. This causes Φ, the outlet air RH, to increase initially and then to decrease. It also can be seen that the area under the negative $\dot{\Phi}$ (from t=3.1 to infinity) is larger than that

under the positive $\dot{\Phi}$. This causes the steady-state value of Φ to become lower than the initial value, thus exhibits a NMP behavior as shown in plot 4 of Fig.7.

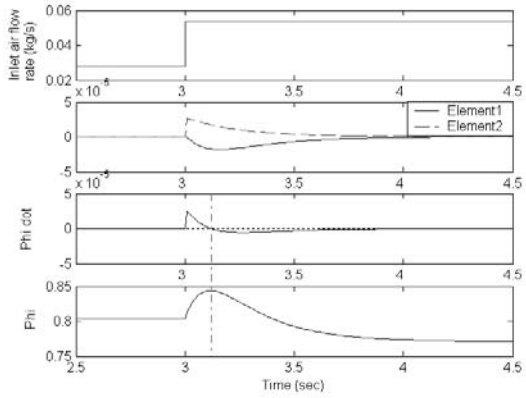

Fig. 7: Air outlet RH and RH rate responses under an inlet air flow rate step increase

We have explained the NMP behavior of Φ, and will establish the connection to the NMP response of $\dot{m}_{v,tr}$ next. The membrane vapor transfer rate $\dot{m}_{v,tr}$ is a function of Φ, as explained in Eqs. (10)-(14). Since the water temperature changes slowly compared with other dynamic variables of the humidifier, $T_{2,out}$ is assumed to be constant. In addition, since the membrane is submerged in water, $T_{mem} = T_{2,out}$. Therefore, the membrane coefficient of diffusion D_w can be viewed as a constant, denoted as D_c. Since water flows through Control Volume 2, λ_2 equals 14 [19]. Substituting λ_2, D_c and Eq. (12), Eq. (10) becomes

$$\dot{m}_{v,tr} = \frac{D_c M_v A \rho_{m,dry}}{t_m M_{m,dry}} (14 - \lambda_1) \tag{25}$$

where $\frac{D_c M_v A \rho_{m,dry}}{t_m M_{m,dry}}$ is constant and $\dot{m}_{v,tr}$ depends on $-\lambda_1$ linearly. The nonlinear relationship between λ_1 and the relative humidity Φ is shown in Fig. 8. Since λ_1 is a monotonic function of RH, if RH has a NMP response, λ_1 will also exhibit a NMP response. Therefore, $\dot{m}_{v,tr}$, which depends linear with λ_1, will exhibit a NMP response.

The root locus plot of the linearized system shown in Fig. 9 confirms this finding. Fig. 9 shows that there is a slow dynamic mode corresponding to the slow pole-zero pair. This slow dynamic mode arises from the water temperature dynamics, which has a large thermal capacitance. Assuming the water temperature is constant, the state $T_{2,out}$ can be eliminated. The system order is then reduced from 4 to 3. When the system input is the inlet air flow rate and the system output is the membrane vapor transfer rate, the linearized transfer function can be expressed as

$$H(s) = \frac{k(s+z_1)(s+z_2)}{(s+p_1)(s+p_2)(s+p_3)} \tag{26}$$

where, p_1, p_2, p_3 and $z_1 > 0$ and $z_2 < 0$. The open loop system has a NMP zero.

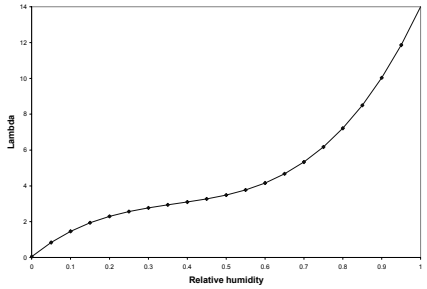

Fig. 8: Lambda vs. gas relative humidity

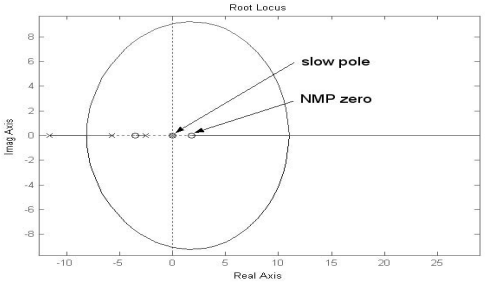

Fig. 9: Root locus of the 4 states system with the inlet air flow rate as the system disturbance

This NMP zero is not desirable because it imposes fundamental limits on the achievable feedback control performance, sensitivity, and robustness properties of a linear time invariant feedback system [20]. It also places an upper limit on the bandwidth achieved by the closed-loop. The further the distance between the NMP zero and the origin is, the higher the possible bandwidth will be [21]. The selection of system parameters, such as the membrane thickness, channel cross section dimension and heat transfer efficiency, could affect the NMP zero location, which then determines the system available bandwidth.

Assuming all other system parameters are constant, the effect of membrane thickness on the NMP zero location is studied. The result is summarized in table 1. The membrane thickness hardly affects the NMP zero value. However, thinner membranes usually result in higher vapor transfer rates and thus are preferred over thicker membranes.

TABLE 1: NMP ZERO VALUE VS. MEMBRANE THICKNESS

Membrane thickness (cm)	NMP zero
0.005	21.08
0.0125	20.71
0.0175	20.64

Assuming all other system parameters are constant, the effect of channel cross section dimension on the NMP zero location is investigated. The results are summarized in table

2, which shows that smaller hydraulic diameters are preferred.

TABLE 2: NMP ZERO VALUE VS. HYDRAULIC DIAMETER

Hydraulic diameter (m)	NMP zero
0.001	21.08
0.002	8.95
0.003	6.44
0.004	5.3

Next we relax the assumption that the humidifier is well insulated and assume the insulation condition can be a design factor. Eq. (18) becomes

$$\dot{Q}_1 = UA\Delta T_{2/1}\eta_0 \tag{27}$$

where η_0 represents the insulation efficiency ($0<\eta_0<1$). Assuming all other system parameters are fixed, the effect of insulation efficiency on the NMP zero location is analyzed. The results are summarized in table 3, which shows that higher insulation efficiency is preferred. Higher insulation efficiency can be achieved by better insulation of the humidifier.

TABLE 3: NMP ZERO VALUE VS. HEAT TRANSFER EFFICIENCY

Insulation efficiency	NMP zero
0.8	21.08
0.6	14.87
0.4	10.48

IV. CONCLUSIONS

A lumped thermodynamic model of membrane-based humidifiers was developed. This model captures the humidification behavior accurately and maintains its simplicity. Dynamic simulation result shows that the system exhibits a non-minimum phase behavior under inlet air flow rate disturbance. This is due to the response lag of the total vapor mass inside the humidifier. The humidifier design parameters, which affect the non-minimum phase zero location in the right-half plane are analyzed. The results show that a system with smaller hydraulic diameter and better insulation produces NMP zeros further away from the origin, i.e., they impose less constraint on closed-loop control performance.

REFERENCES

[1] K. Broka and P. Ekdunge, *Oxygen and Hydrogen Permeation Properties and Water Uptake of Nafion 117 Membrane and Recast Film for PEM Fuel Cell*, Sweden, Chapman & Hall, 1997.

[2] J. St-Pierre, D.P. Wilkinson, S. Knights and M. Bos, Relationships between Water Management, "Contamination and Lifetime Degradation in PEFC", *Journal of New Materials for Electrochemical Systems*, v.3, pp.99-106, 2000.

[3] T.J.P. Freire and E.R. Gonzalez, "Effect of Membrane Characteristics and Humidification Conditions on the Impedance Response of Polymer Electrolyte Fuel Cells", *Journal of Electroanalytical Chemistry*, v.503, pp.57-68, 2001.

[4] D. Chu and R.Z. Jiang, "Performance of Polymer Electrolyte Membrane Fuel Cell (PEMFC) Stacks Part I. Evaluation and Simulation of an Air-Breathing PEMFC Stack", *Journal of Power Sources*, 83, pp.128-pp.133, 1999.

[5] T.H. Yang, Y.G. Yoon, C.S. Kim, S.H. Kwak and K.H. Yoon, "A Novel Preparation Method of a Self-humidifying Polymer Electrolyte Membrane", *Journal of Power Source*, v.106, pp.328-332, 2002.

[6] D. Staschewski and Z.Q. Mao, "Hydrogen-Air PEMFC Operation with Extraordinarily Low Gas Pressures and Internal Humidification-Conception and Experimental Prototype Stack", *International Journal of Hydrogen Energy*, v.24, pp.543-548, 1999.

[7] T.E. Springer, T.A. Zawodzinski and S. Gottesfeld, "Polymer Electrolyte Fuel Cell Model", *Journal of Electrochemical Society*, v.138, No.8, pp.2334-2342, 1991.

[8] S. Um, C.-Y. Wang, and K.S. Chen, "Computational Fluid Dynamics Modeling of Proton Exchange Membrane Fuel Cells", *Journal of The Electrochemical Society*, 147 (12) pp.4485-4493, 2000.

[9] S. Shimpalee and S. Dutta, "Numerical Prediction of Temperature Distribution in PEM Fuel Cells", *Journal of Numerical Heat Transfer*, Part A, v.38, pp.111-128, 2000.

[10] L. Pisani, G. Murgia, M. Valentini and B. D'Aguanno, "A Working Model of Polymer Electrolyte Fuel Cells-Comparisons between Theory and Experiments", *Journal of the Electrochemical Society*, v.149, No.7, pp.898-904, 2002.

[11] J.J. Baschuk and X. Li, "Modeling of Polymer Electrolyte Membrane Fuel Cells with Variable Degrees of Water Flooding", *Journal of Power Sources*, v.86, pp.181-196.

[12] M. Ceraolo, C. Miulli and A. Pozio, "Modelling Static and Dynamic Behavior of Proton Exchange Membrane Fuel Cells on the Basis of Electro-chemical Description", *Journal of Power Sources*, v.113, pp.131-144, 2003.

[13] G.J.M. Janssen and M.L.J. Overvelde, "Water Transport in the Proton-Exchange-Membrane Fuel Cell: Measurements of the Effective Drag Coefficient", *Journal of Power Sources*, v. 101, pp.117-125, 2001.

[14] T.V. Nguyen and R.E. White, "A Water and Heat Management-Membrane Fuel Cells", *Journal of Electrochemical Society*, v.140, No.8, pp.2178-2186, 1993.

[15] D. Picot, R. Metkemeijer, J.J. Bezian and L. Rouveyre, "Impact of the Water Symmetry Factor on Humidification and Cooling Strategies for PEM Fuel Cell Stacks", *Journal of Power Sources*, v.75, p.251-p.260, 1998

[16] P. Sridhar, R. Perumal, N. Rajalakshmi, M. Raja and K.S. Dhathathreyan, "Humidification Studies on Polymer Electrolyte Membrane Fuel Cell", *Journal of Power Sources*, v.101, pp.72-78, 2001.

[17] K.H. Choi, D.J. Park, Y.W. Rho, Y.T. Kho and T.H. Lee, "A Study of the Internal Humidification of An Integrated PEMFC Stack", *Journal of Power Sources*, v.74, pp.146-150, 1998.

[18] F.N. Buchi and S. Srinivasan, "Operating Proton Exchange Membrane Fuel Cells without External Humidification of the Reactant Gases-Fundamental Aspects", *Journal of Electrochemical Society*, v.144, No.8, pp.2767-2772, 1997.

[19] D. Chen and H. Peng, "Modeling and Simulation of a PEM Fuel Cell Humidification System", *Proceeding of 2004 American Control Conference*, Boston, Massachusetts.

[20] R.H. Middleton, J.S. Freudenberg and N.H. McClamroch, "Sensitivity and Robustness Properties in the Preview Control of Linear Non-Minimum Phase Plants", *Proceedings of the American Control Conference*, Arlington, VA. June 25-27, 2001.

[21] R.H. Middleton, "Trade-offs in Linear Control System Design", *Automatica*, v. 27, No. 2, pp. 281-292, 1991.